

1 Automated ambiguity estimation for VLBI Intensive
2 sessions using L1-norm

3 Niko Kareinen, Thomas Hobiger, Rüdiger Haas

4 *Chalmers University of Technology*
5 *Department of Earth and Space Sciences*
6 *SE-412 96 Gothenburg*
7 *Sweden*

8 **Abstract**

9 Very Long Baseline Interferometry (VLBI) is a space-geodetic technique that
10 is uniquely capable of direct observation of the angle of the Earth's rotation
11 about the Celestial Intermediate Pole (CIP) axis, namely UT1. The daily
12 estimates of the difference between UT1 and Coordinated Universal Time
13 (UTC) provided by the 1-hour long VLBI Intensive sessions are essential in
14 providing timely UT1 estimates for satellite navigation systems and orbit
15 determination. In order to produce timely UT1 estimates, efforts have been
16 made to completely automate the analysis of VLBI Intensive sessions. This
17 involves the automatic processing of X- and S-band group delays. These data
18 contain an unknown number of integer ambiguities in the observed group
19 delays. They are introduced as a side-effect of the bandwidth synthesis tech-
20 nique, which is used to combine correlator results from the narrow channels
21 that span the individual bands. In an automated analysis with the c5++
22 software the standard approach in resolving the ambiguities is to perform a
23 simplified parameter estimation using a least-squares adjustment (L2-norm
24 minimisation). We implement L1-norm as an alternative estimation method

25 in c5++. The implemented method is used to automatically estimate the
26 ambiguities in VLBI Intensive sessions on the Kokee–Wettzell baseline. The
27 results are compared to an analysis set-up where the ambiguity estimation
28 is computed using the L2-norm. For both methods three different weighting
29 strategies for the ambiguity estimation are assessed. The results show that
30 the L1-norm is better at automatically resolving the ambiguities than the
31 L2-norm. The use of the L1-norm leads to a significantly higher number of
32 good quality UT1-UTC estimates with each of the three weighting strate-
33 gies. The increase in the number of sessions is approximately 5 % for each
34 weighting strategy. This is accompanied by smaller post-fit residuals in the
35 final UT1-UTC estimation step.

36 *Keywords:* Earth rotation, UT1, VLBI, automated analysis, robust
37 estimation

38 1. Introduction

39 Very Long Baseline Interferometry (VLBI) is a unique technique among
40 space-geodetic techniques due to its capability to determine all Earth Ori-
41 entation Parameters (EOP) simultaneously. These parameters provide the
42 orientation of the Earth in an inertial reference system. One of the parame-
43 ters is the Earth’s rotation about the Celestial Intermediate Pole (CIP) axis,
44 which is described as Universal Time (UT1). VLBI measures the difference
45 between the UT1 and Universal Coordinated Time (UTC), UT1-UTC, from
46 which the UT1 can subsequently be estimated.

47 By monitoring Earth rotation it is possible to gather information about
48 the underlying geodynamical behaviour of the Earth system. Thus, also UT1

49 as a parameter is connected to various geophysical phenomena, in particular
50 via the exchange of angular momentum between the atmosphere, geophysical
51 fluids, and the solid earth (Barnes et al., 1983). Thus, high-frequency signals
52 in UT1 can be used to study these geophysical excitations and the under-
53 lying geodynamical phenomena (Brzeziński, 2012). Moreover, the impact of
54 earthquakes with large magnitude, such as the Denali earthquake in 2002,
55 has also been verified by EOP parameters (Titov and Tregoning, 2005), and
56 therefore stresses the need for real-time EOP monitoring.

57 Furthermore, timely UT1 estimates from VLBI are crucial for space-
58 geodetic techniques such as Global Satellite Navigation Systems (GNSS).
59 GNSS are only capable of accessing UT1 via its time derivative, usually de-
60 noted as the change in Length-of-Day (LOD), and rely on UT1 input from
61 VLBI.

62 The International VLBI Service for Geodesy and Astrometry (IVS)
63 (Behrend, 2013) organises daily 1-hour long VLBI observing sessions called
64 the Intensive sessions (INT). Characteristic to these sessions is that they are
65 observed on extended East–West-baselines using a network of 2 to 3 antennas.
66 Currently three types of INT sessions are conducted regularly. INT1 are
67 observed on the Kokee (Hawaii) – Wettzell (Germany) baseline from Monday
68 to Friday at 18:30 UTC. INT2 are observed on the Tsukuba (Japan) –
69 Wettzell (Germany) baseline on Saturday and Sunday at 7:30 UTC. Finally,
70 to fill in the gap between the last INT2 of the week and the first INT1, INT3
71 are observed with a network consisting of Wettzell, Tsukuba, and Ny-Ålesund
72 on Monday mornings at 7:00 UTC. The short duration of the sessions and
73 the baseline geometry leads to a relatively low number of approximately 20–

74 40 observations per baseline. The aim of the INT sessions is to produce
75 daily UT1 estimates in a timely fashion. The turnaround time of the results
76 depends on the VLBI processing chain. Namely, the time it takes to correlate
77 the observed data to produce databases, which are subsequently analysed
78 by various VLBI analysis packages in order to obtain the UT1 estimates.
79 One way to streamline this analysis chain is to automatically process the
80 correlated data. Automated near-real time analysis of INT sessions has been
81 investigated in e.g. Hobiger et al. (2010) and Kareinen et al. (2015).

82 Geodetic VLBI sessions are typically observed on two frequency bands
83 centred around 8.4 GHz (X-band) and 2.3 GHz (S-band). A linear combina-
84 tion of the observed delays on the two bands can be used to derive a delay
85 observable that is almost completely free of ionospheric effects. The two
86 bands consist of individual channels, which are in the post-correlation proce-
87 dure combined with a bandwidth synthesis technique (Rogers, 1970) to span
88 the whole bandwidth. A side-effect of this procedure is that an unknown
89 number of integer ambiguities are introduced into the observed group delays.
90 The ambiguities are proportional to the channel spacing within the individ-
91 ual bands. For a typical channel set-up in an INT session these ambiguities
92 are 50 ns for X-band and 200 ns for S-band. For comparison, the formal er-
93 rors for the observed delays in the correlator output for the INT sessions are
94 approximately three orders of magnitude smaller. Before the ionospheric cal-
95 ibration can be computed, the ambiguities have to be resolved on each band.
96 Any unresolved ambiguities in the observed group delays will propagate into
97 the UT1 estimates.

98 There are multiple available VLBI software packages which can be used

99 to estimate geodetic parameters from VLBI observations. These include e.g.
100 c5++ (Hobiger et al., 2010), CALC/SOLVE (Ma et al., 1990), Vienna VLBI
101 Software (VieVS) (Böhm et al., 2012), GEOSAT (Andersen, 2000), OCCAM
102 (Titov et al., 2004), and OCCAM/GROSS (Malkin and Skurikhina, 2005).
103 A recent modernisation for the SOLVE part in CALC/SOLVE is ν Solve
104 (Bolotin et al., 2014). Out of these software packages, c5++, CALC/SOLVE,
105 and ν Solve are the only ones that allow to resolve the group delay am-
106 biguities to produce ambiguity- and ionosphere-free X-band databases. The
107 databases produced by the correlator contain group delays which include am-
108 biguities and ionospheric effects. These databases are referred to as Version-1
109 databases.

110 The standard approach for parameter estimation in all software packages
111 mentioned above is the method of least-squares adjustment (Koch, 1999)
112 (i.e. L2-norm minimisation). In this paper, as an alternative approach to
113 the L2-norm, we implement parameter estimation based on the L1-norm and
114 apply it to the analysis of the INT sessions in the ambiguity resolving step.
115 Furthermore, we evaluate alternative weighting strategies for both the L1-
116 and L2-norm ambiguity estimation. Compared to the L2-norm, the L1-norm
117 should be more robust in the presence of outliers. We investigate whether
118 this robust estimator helps to correctly detect the ambiguities in the initial
119 stages of the analysis process. Starting from Version-1 databases we use the
120 modified c5++ to automatically analyse INT1 sessions from 2001 to 2015 to
121 estimate UT1.

122 **2. Formulation of the minimisation conditions**

123 The objective functions for both the L1- and L2-norm minimisations can
124 be derived from the general expression for a p-norm, which is given by

$$125 \quad ||x||_p = \left(\sum_{i=1}^p |x_i|^p \right)^{\frac{1}{p}}. \quad (1)$$

126 The L1-norm and L2-norms correspond to Equation 1 with p-values of
127 p=1 and p=2, respectively. In both cases the norms to be minimized are
128 functions of the residuals v_i between the functional model and the observa-
129 tions, as well as possible weighting terms. The weight terms are included as
130 multiplicative factors in the summands of the norms. Thus for, L1 and L2
131 the objective functions to be minimised are given respectively by

$$132 \quad \text{L1} : \min(\mathbf{p}^\top |\mathbf{v}|), \quad (2)$$

$$133 \quad \text{L2} : \min(\mathbf{v}^\top \mathbf{P} \mathbf{v}), \quad (3)$$

134 where \mathbf{v} is a vector containing the residuals for n observations, \mathbf{p} is a
135 vector containing the associated weights for the observations, and \mathbf{P} is an
136 $n_{\text{obs}} \times n_{\text{obs}}$ matrix in which the diagonal contains the weights for the obser-
137 vations and the off-diagonal elements the possible correlation terms.

138 In the following subsections, first the standard L2-norm minimisation
139 procedure is described. Then the derivations of the equations needed to
140 solve the L1-norm minimisation problem are discussed.

141 *2.1. L2-norm minimisation*

142 A detailed description of the L2-norm minimisation can be found in e.g.
143 Koch (1999). Generally, the L2-norm minimisation is done according to the

144 condition given by Equation 3. A linear functional model in matrix form is
145 given by

$$146 \quad \mathbf{v} = \mathbf{Ax} - \mathbf{y}, \quad (4)$$

147 where \mathbf{v} is the residual vector, \mathbf{A} is the design matrix, \mathbf{x} is the vector
148 containing the unknown parameters of the model, and \mathbf{y} is the observation
149 vector. The design matrix \mathbf{A} contains information on how the unknown
150 variables relate to the observations in the functional model. Often the initial
151 functional model of the system in question is not linear. In this case the
152 system needs to be linearised. In a linearised system the design matrix will
153 contain the partial derivatives of the model with respect to the unknown
154 parameters. Using the expression for the residuals given by Equation 4 in
155 Equation 3, we can write the weighted sum of the residuals as

$$156 \quad \mathbf{v}^T \mathbf{P} \mathbf{v} = (\mathbf{Ax} - \mathbf{y})^T \mathbf{P} (\mathbf{Ax} - \mathbf{y}) \quad (5)$$

157 Differentiating the expression in Equation 5 with respect to \mathbf{x} and setting
158 it to equal 0 we obtain

$$159 \quad \hat{\mathbf{x}} = (\mathbf{A}^T \mathbf{P} \mathbf{A})^{-1} \mathbf{A}^T \mathbf{P} \mathbf{y}. \quad (6)$$

160 From Equation 6 we obtain the vector of unknowns, which will minimise
161 the squared sum of the weighted residuals. An important property of the
162 L2-norm is that the absolute value term in the sum is squared, and thus
163 the absolute value function can be omitted. This enables us to differentiate
164 the expression given in Equation 5. Thus, the L2-norm is computationally
165 straightforward, with the most costly operation being the matrix inversion

166 in Equation 6. In the case of the L1-norm the differentiability is an issue
 167 and requires an alternative approach. The standard parameter estimation
 168 in the c5++ analysis software is based on iterative least-squares (L2-norm)
 169 minimisation.

170 *2.2. L1-norm minimisation*

171 The L1-norm minimisation, which is discussed in detail in e.g. Koch
 172 (1999), starts from the same functional model set-up used in Equation 4.
 173 However, now the residual vector \mathbf{v} remains inside the absolute value func-
 174 tion. Consequently, it is not differentiable at 0, and we are unable to derive
 175 the value for the vector of unknowns \mathbf{x} that will minimise the sum of the
 176 weighted absolute values of the residuals. The formulation for a L1-norm
 177 minimisation has been described in e.g. Amiri-Simkooei (2003). Following
 178 this general formulation, in order to deal with absolute value function in the
 179 Equation 2, we re-write the vectors \mathbf{v} and \mathbf{x} with the help of slack variables.
 180 This will reduce the problem to that of a linear programming. These vectors
 181 are now given by

182
$$\mathbf{v} = \mathbf{u} - \mathbf{w}, \quad \mathbf{u}, \mathbf{w} \geq 0, \quad (7a)$$

183
$$\mathbf{x} = \boldsymbol{\alpha} - \boldsymbol{\beta}, \quad \boldsymbol{\alpha}, \boldsymbol{\beta} \geq 0, \quad (7b)$$

 184

185 where a condition u_i or $w_i = 0$ holds for the residual vector components.
 186 Now given the conditions in Equation 7a, Equation 2 can be written as

187
$$\mathbf{p}^\top |\mathbf{v}| = \mathbf{p}^\top |\mathbf{u} - \mathbf{w}| = \mathbf{p}^\top (\mathbf{u} + \mathbf{w}), \quad (8)$$

188 subject to the conditions in Equation 7b,

189
$$\mathbf{u} - \mathbf{w} = \mathbf{A}(\boldsymbol{\alpha} - \boldsymbol{\beta}) - \mathbf{y}. \tag{9}$$

190 The objective function can now be written as

191
$$\min \left(\begin{array}{c} \left[\mathbf{0}^T \quad \mathbf{0}^T \quad \mathbf{p}^T \quad \mathbf{p}^T \right] \begin{bmatrix} \boldsymbol{\alpha} \\ \boldsymbol{\beta} \\ \mathbf{w} \\ \mathbf{u} \end{bmatrix} \end{array} \right), \tag{10}$$

192 subject to

193
$$\left[\mathbf{A} \quad -\mathbf{A} \quad \mathbf{I} \quad -\mathbf{I} \right] \begin{bmatrix} \boldsymbol{\alpha} \\ \boldsymbol{\beta} \\ \mathbf{w} \\ \mathbf{u} \end{bmatrix} = \mathbf{y}, \tag{11}$$

194 given the same conditions as earlier. Denoting the objective function with
 195 z this form is equivalent to

196
$$z = \mathbf{c}^T \mathbf{x}, \tag{12}$$

197 subject to

198
$$\mathbf{A}\mathbf{x} = \mathbf{b}, \quad \mathbf{x} \geq 0. \tag{13}$$

199 The L1-norm minimisation was implemented in c5++ as an external
 200 python script. The corresponding linear programming problem was solved
 201 using a Simplex-method (Murty, 1983) implemented in the *linprog* function
 202 of the optimisation module in SciPy (Walt et al., 2011).

203 *2.3. Theoretical comparison of L1- and L2-norm*

204 Generally, the advantage of the L2-norm is that it is computationally
205 simple. The L2-norm is intrinsically stable and it has a unique solution. Fur-
206 thermore, if the measurement errors are assumed to be normally distributed
207 around 0 with a variance of σ^2 , the L2-norm is the maximum likelihood es-
208 timator (MLE) for the unknowns. Thus, for normally distributed errors, the
209 L2-norm will give the optimal estimates for the unknowns. However, as-
210 suming normality might not always be justified, and it can be hard to infer
211 from the results whether the assumption was in fact correct. The sampling
212 variance of the L2-norm is proportional to σ^2/n , where n is the sample size.
213 Even though the L2-norm is efficient, its disadvantage is its sensitivity to
214 outliers. Because the sum deals with squared residuals, large deviations in
215 the residuals tend to have high impact on the overall sum. This in turn will
216 propagate into the unknowns.

217 Compared to the L2-norm, the main advantage of the L1-norm is its
218 increased robustness against outliers. Since the L1-norm sums absolute devi-
219 ations instead of squared values, large residuals do not influence the solution
220 to the same degree as with the L2-norm. Consequently, the L1-norm will
221 more likely correctly detect the magnitude of the large outliers, instead of
222 propagating the error into the unknowns through the adjustment. The L2-
223 norm tends to overcompensate the influence of large deviations. For example,
224 in case of a simple linear regression, by shifting the regression line towards
225 the outliers, making the individual residual smaller but consequently provid-
226 ing a worse fit for the good observations. With the L1-norm large deviations
227 do not dominate the sum to a same degree, and thus in case of e.g. linear

228 regression, the fit is not shifted towards the erroneous observation as much,
229 keeping the residuals of the good observations smaller and correctly detecting
230 the magnitude of the bad one.

231 However, the L1-norm has some clear disadvantages compared to the
232 L2-norm, as well. Firstly, the solution is not always stable and there is
233 no guarantee of a unique solution. In contrast to the MLE condition of
234 the L2-norm, the L1-norm is the MLE when the errors follow a Laplace
235 distribution with μ and b as the location and scale parameters. In case of
236 normally distributed errors $e \sim N(0, \sigma^2)$ the sampling variance for L1-norm
237 is proportional to $(\pi/2)(\sigma^2/n)$ (Andersen, 2008). Thus, if the errors are in
238 general normally distributed, the L1-norm will likely produce larger variance
239 compared to the L2-norm.

240 Keeping these considerations in mind, the L1-norm has the potential to
241 be very effective in detecting outlier of large magnitude. This corresponds
242 well to the case of the ambiguity resolution problem in geodetic VLBI where
243 the ambiguities have far greater magnitude than the overall noise-floor of the
244 observations.

245 **3. Automated ambiguity estimation for Intensive sessions**

246 To investigate the performance of the L1-norm in the ambiguity estima-
247 tion we analysed a total of 1835 INT1 sessions observed in the period of
248 2001–2015, starting from Version-1 databases. The sessions were analysed
249 in automated mode by resolving the ambiguities with both the L1- and L2-
250 norm approach. The ambiguity-resolved databases were then subsequently
251 processed to estimate the UT1-UTC with respect to the EOP product of

252 International Earth Rotation and Reference Frame Service (IERS), namely
253 EOP C04 08 (Bizouard and Gambis, 2011). This latter estimation was car-
254 ried out using the standard L2-norm method for both ambiguity resolving
255 methods. Thus, the only differences to the analysis due to the L1- and L2-
256 norms are introduced in the ambiguity estimation step.

257 *3.1. Ambiguity estimation in c5++*

258 The general ambiguity estimation process in c5++ is iterative. The X-
259 and S-band group delays are processed as independent observations, which
260 retains the integer-nature of the ambiguities. In contrast, the software pack-
261 age SOLVE (Ma et al., 1990), which has long been used operatively for the
262 IVS data products, combines the X- and S-band group delays in the ini-
263 tial stage of the automated ambiguity estimation. The modern replacement
264 for Solve, ν Solve (Bolotin et al., 2014), implements similar concepts in its
265 automated group delay ambiguity estimation.

266 The functional model used for the ambiguity resolution in c5++ is de-
267 scribed in Hobiger et al. (2010). In general, the model includes a quadratic
268 polynomial for the station clock behaviour, an offset term between X- and
269 S-band to consider inter-band instrumental delays, and the troposphere de-
270 lays at each station. One of the stations is always chosen as the reference,
271 for which the clock and inter-band offsets are not estimated. Thus, in the
272 case of INT1 and one baseline we estimate in total three clock coefficients
273 and the band offset term for the non-reference station. In this analysis the
274 troposphere parameters were also estimated. The troposphere parameters at
275 the stations are estimated to the zenith-direction and mapped to the source
276 elevation using a mapping function. There are multiple mapping functions

277 available. In this analysis we used the Global Mapping Functions (GMF2)
 278 together with Global Pressure and Temperature Model (GPT2) (Lagler et al.,
 279 2013).

280 In each iteration step the residuals are computed and if they are larger
 281 than 50 % of the ambiguity spacing on that band, the corresponding ob-
 282 servations are shifted by one ambiguity spacing towards 0. This process of
 283 ambiguity shifting is iterated until the ratio of the WRMS values of the resid-
 284 uals from subsequent iterations reaches a pre-specified level. This level was
 285 set to 0.999 in all our analyses which are discussed hereafter. The maximum
 286 number of iterations was set to 60. During the estimation process, different
 287 weighting schemes can be applied. The effect of the choice of weighting was
 288 investigated using three different approaches, which are described in Table 1.

Table 1: The three different weighting approaches used in the ambiguity estimation.

Weighting mode	Description	Weighting
W1	Unit weighting	1
W2	Formal errors	$\frac{1}{\sigma_\tau^2}$
W3	Formal errors multiplied by wet mapping functions values (elevation dependent)	$\frac{1}{\sigma_\tau^2(\text{mf}(e)_{\text{wet},1}^2 + \text{mf}(e)_{\text{wet},2}^2)}$

289 Once the ambiguities are resolved, the X- and S-band data are combined
 290 to produce an ionosphere free X-band database. This database is then sub-

291 sequently used as an input in the UT1-UTC estimation step. In this step the
 292 observations were weighted according to the elevation dependent approach,
 293 W3. The schematics in Figure 1 illustrate the ambiguity and UT1-UTC
 294 estimation process in c5++.

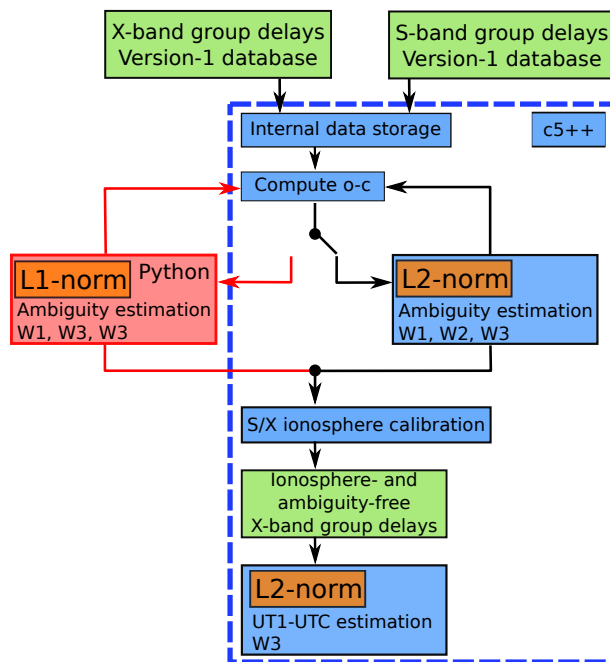


Figure 1: Schematics of the automated ambiguity and UT1-UTC estimation in c5++.

295 3.2. Indicators for successfully resolved ambiguities

296 In order to assess whether the ambiguities have indeed been successfully
 297 resolved, we need to define criteria, that capture the effect of the ambiguity
 298 estimation.

299 Since any unresolved ambiguities will propagate into the estimated pa-
 300 rameters, a straightforward method is to investigate the UT1-UTC estimates
 301 obtained from the two ambiguity estimation approaches. In this estimation

302 step the station coordinates were kept fixed to their a priori ITRF2008 (Al-
303 tamimi et al., 2011) values. Except UT1-UTC, all EOP were fixed to their
304 EOP C04 08 values. The UT1-UTC were estimated with respect to the a pri-
305 ori C04 08 values. From now on these values will be referenced simply as
306 the UT1-UTC estimates. In addition to UT1-UTC, a quadratic clock for the
307 non-reference stations and the wet troposphere for both stations were esti-
308 mated. This set-up is typical for INT sessions, since due to the combination
309 of short session duration and baseline geometry, the only EOP that can be
310 viably determined is UT1-UTC.

311 Furthermore, we can directly compare the Root Mean Square (RMS) and
312 Weighted RMS (WRMS) values for the post-fit residuals from the ambiguity
313 resolution runs. In the ambiguity resolution step no outlier elimination is
314 performed, because in the presence of ambiguities every observation has the
315 potential to be interpreted as an outlier. Thus, any unresolved ambiguities
316 will be reflected as higher RMS and WRMS values. In the UT1-UTC esti-
317 mation step in c5++, 3- σ outliers are detected at iteration step i following
318 an empirically derived condition (Hobiger et al., 2010)

$$319 \quad |o - c|_i > \text{WRMS}_{i-1} \frac{3}{\sqrt{2}} \sqrt{\text{mf}(e)_{\text{wet},1}^2 + \text{mf}(e)_{\text{wet},2}^2} \Rightarrow \text{outlier}, \quad (14)$$

320 where the $o - c$ is the difference between the observed and computed
321 value at the i th iteration, WRMS_{i-1} is the WRMS value from the previous
322 iteration, and $\text{mf}_{\text{wet},1}^2$ and $\text{mf}_{\text{wet},2}^2$ are the wet mapping function values for
323 the stations 1 and 2, respectively. This outlier detection algorithm implies
324 that if the WRMS from the previous iteration is high, the solution is more
325 tolerant to large residuals.

326 4. Results

327 The impact of using the L1-norm in the ambiguity estimation was exam-
328 ined by investigating the criteria described in Section 3.2. In order to focus
329 on the sessions which produced meaningful UT1-UTC estimates w.r.t C04
330 and to eliminate gross errors that would distort the derived statistics of the
331 UT1-UTC, the estimates, meaning the adjustments to the a priori values,
332 were filtered with a condition where the absolute values of the estimates are
333 larger than 1000 μs and/or the formal errors are larger than 50 μs . After
334 this initial outlier elimination was applied, we obtained a set of sessions for
335 each ambiguity estimation method–weighting mode pair, for which RMS and
336 WRMS of the UT1-UTC values were computed. These values are listed in
337 Table 2. The largest number of good sessions is highlighted for each weight-
338 ing strategy. The RMS and WRMS values for the post-fit residuals from the
339 ambiguity estimation for both norms and all weighting strategies are listed
340 in Table 3.

341 The results in Table 2 show that the RMS and WRMS values of the
342 UT1-UTC estimates for both approaches are very close. The differences
343 in all categories are below 0.2 μs . These values reflect the general level of
344 UT1-UTC accuracy obtainable from INT sessions (Kareinen et al., 2015).
345 The noteworthy conclusion is that the L1-norm gives a larger number of
346 good sessions compared to the L2-norm, and this is true for all weighting
347 strategies. The largest difference is seen with weighting W1, where the L1-
348 norm approach to resolve ambiguities produces 84 more good sessions. The
349 L1-norm resulted in an increase of 5.4 %, 4.4 %, and 4.6 % for the number
350 of good sessions using the W1, W2, and W3 weightings, respectively.

Table 2: Impact of the weighting strategies for ambiguity estimation on final UT1-UTC results. Presented are the number of sessions and corresponding RMS/WRMS of UT1-UTC values w.r.t. C04 for the sessions, which pass the $|\text{UT1-UTC}| < 1000 \mu\text{s}$ and $\sigma_{\text{UT1-UTC}} < 50 \mu\text{s}$ criteria. For each weighting strategy the highest number of sessions between the L1- and L2-norm approaches are highlighted in boldface.

	L1			L2		
	#Sessions	RMS [μs]	WRMS [μs]	#Sessions	RMS [μs]	WRMS [μs]
W1	1649	22.58	18.39	1565	22.58	18.37
W2	1469	22.32	18.43	1407	22.50	18.53
W3	1493	22.25	18.43	1428	22.42	18.37

Table 3: Mean RMS and WRMS of the post-fit residuals from the ambiguity estimation for L1- and L2-norms for all weighting strategies.

	L1		L2	
	$\overline{\text{RMS}}$ [m]	$\overline{\text{WRMS}}$ [m]	$\overline{\text{RMS}}$ [m]	$\overline{\text{WRMS}}$ [m]
W1	1.08	1.08	1.25	1.25
W2	1.87	0.42	1.86	0.51
W3	1.83	0.37	1.87	0.43

351 The mean RMS and WRMS of the post-fit residuals presented in Table 3
352 show that the L1-norm gives on average a better fit after the ambiguity
353 estimation. The only exception is weighting W2 where the RMS of the L2-
354 norm is smaller by 30 ps.

355 The number of iterations that it takes for the ambiguity estimation to
356 converge may reflect both the initial quality of the data, the impact of the
357 weighting method, as well as the stability of the estimation method. The
358 number of iterations for the L1- and L2-norms approaches and weightings
359 W1, W2, and W3 are presented in Figure 2.

360 The success of the ambiguity estimation is reflected in the post-fit group
361 delay residuals from the UT1-UTC estimation. The errors from the unre-
362 solved ambiguities propagate to the estimated parameters during the first
363 iteration of the UT1-UTC estimation. The outlier elimination algorithm in
364 c5++ given in Equation 14 depends on the WRMS of the previous iteration.
365 Parameters estimated in the first iteration bear the risk to absorb outliers
366 and thus subsequent iterations are not able discern between good observa-
367 tions and outliers.

368 Shown in Figure 3 are the residuals for the both L1- and L2-norm ap-
369 proaches and all three weighting strategies. It becomes clear that the residu-
370 als from the L1-norm approach are smaller in general. This can be confirmed
371 both with more L1-residuals located closer to zero and less L1-residuals with
372 large magnitudes.

373 The overlap of the sets of good sessions obtained with the L1- and L2-
374 norm approaches are illustrated by Venn-diagrams in Figure 4. These dia-
375 grams show the number of good sessions which are found in both L1 and L2,

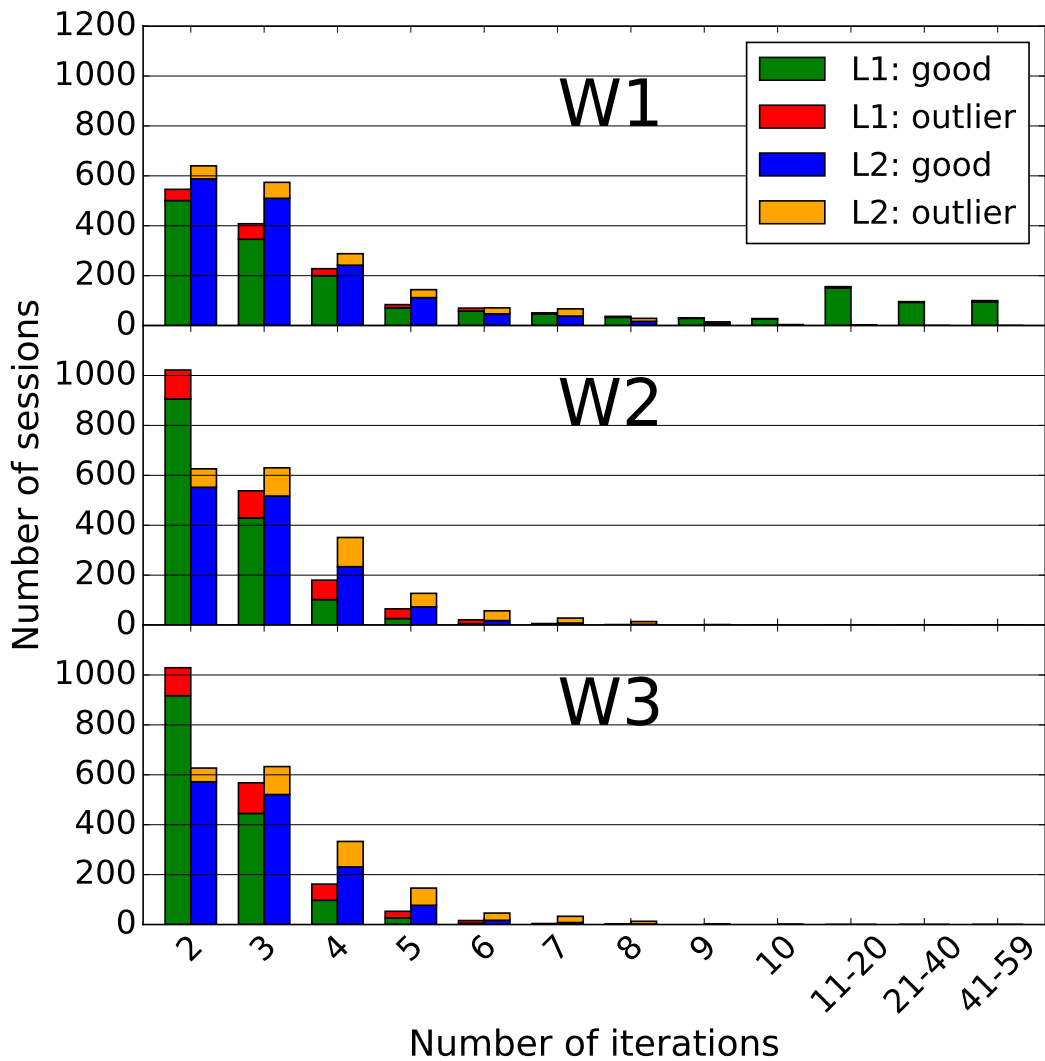


Figure 2: Session distribution by the number of iterations for the L1- and L2-norm approaches for each weighting strategy W1, W2, and W3. The histograms separate between the sessions passing the 1000 μs /50 μs criterion with a different pair of colours for both norms.

376 only L1, or only L2 results.

377 To investigate the sessions that fail with either the L1- or L2-norm ap-

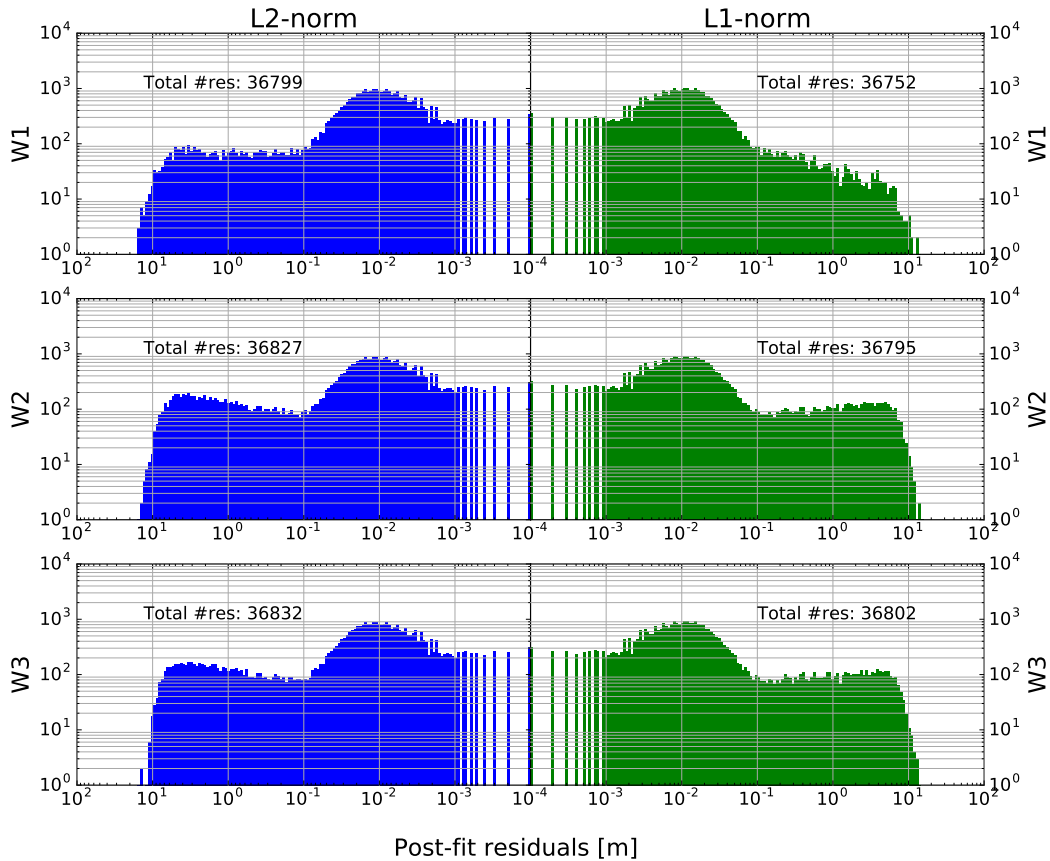
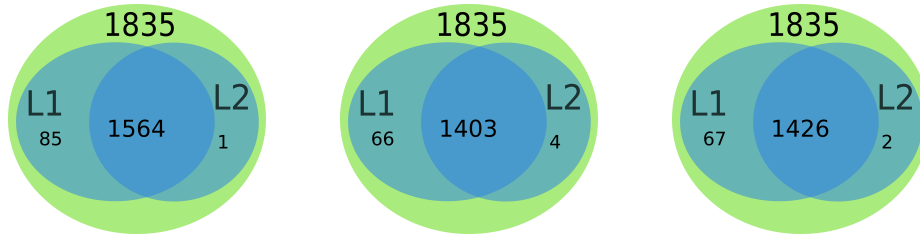


Figure 3: The distribution of the post-fit residuals from UT1-UTC estimation for the L2- (left, blue) and L1-norm (right, green) approaches and weighting strategies W1, W2, and W3.

378 proaches, we consider subsets from all the sessions that resulted in good
 379 UT1-UTC estimate with either approach. In particular, we concentrate on
 380 subsets with the sessions that succeeded with the L1-norm approach. The
 381 following subsets of Figure 4 are considered for all weighting strategies:

- 382 • Subset-1: select all sessions that are good with the L1-norm approach,
 383 select the same sessions from the L2-norm solutions.



(a) Weighting: W1

(b) Weighting: W2

(c) Weighting: W3

Figure 4: Venn-diagrams for the weighting strategies W1, W2, and W3 illustrating the overlap between the sets of sessions obtained with the L1- and L2-norm ambiguity estimation, that pass the $|UT1-UTC| < 1000 \mu s$ and $\sigma_{UT1-UTC} < 50 \mu s$ criteria.

384 – W1: $1564 + 85 = 1649$ sessions

385 – W2: $1403 + 66 = 1469$ sessions

386 – W3: $1426 + 67 = 1493$ sessions

387 • Subset-2: select all sessions that are exclusively good with the L1-norm
388 approach, select the same sessions from the L2-norm solutions.

389 – W1: 85 sessions

390 – W2: 66 sessions

391 – W3: 56 sessions

392 • Subset-3: select all sessions that are exclusively good in the L2-norm
393 approach, select the same sessions from the L1-norm solutions.

394 – W1: 1 session

395 – W2: 4 sessions

396 – W3: 2 sessions

397 The average number of observations (X- or S-band) in the whole set of
398 1835 sessions is 20.5. For the Subset-1 and weighting strategies W1, W2,
399 and W3, the average number of observations are 20.7, 20.8, and 20.8. These
400 values are slightly higher the average number observations of all sessions.
401 This shows that on average sessions with a higher number of observations
402 lead to better UT1-UTC estimate.

403 Similarly, for the Subset-2 the average number of observations are 18.8,
404 20.6, and 20.4. For weighting W2 and W3 the average number of observations
405 between Subset 2 and all sessions are very close to one another. For the
406 weighting W1 the larger number of extra sessions between L1- and L2-norm
407 compared to weightings W2 and W3 correspond to including sessions that
408 have less than average number of observations when compared to the average
409 of all sessions. Thus, with weighting W1 the L2-norm approach fails more
410 often than the L1-norm approach with sessions that had slightly less than
411 average number of observations.

412 The Subset-3 has very few observations in all the weighting strategies
413 W1, W2, and W3. The average number of observations in Subset-3 and
414 weightings W1, W2, and W3, are 16.0, 20.3, and 20.5, respectively. These
415 values are similar to the corresponding Subset-2 results. This indicates that
416 the failure of the L1-norm approach in Subset-3 is not related to the number
417 of observations in these sessions. Furthermore, weighting W1 again has lower
418 than average number of observations. Based on the number of observations
419 in Subset-2 and Subset-3 with weighting W1 the low number of observations
420 cause instability, which the L1-norm approach is able to handle better.

421 Next, we investigate the extent to which the added sessions obtained

422 with the L1-norm approach influences the UT1-UTC accuracy by selecting
 423 the sessions in Subset-1. The results from this comparison are presented
 424 in Table 4. The counterpart to the Subset-1 would be a subset, where we
 425 select the good L2-norm sessions and the same sessions processed with the
 426 L1-norm. However, since there are only a few sessions that have a good
 427 UT1-UTC solution exclusively with the L2-norm, their relative number with
 428 respect to the total number of good sessions is very low. Thus it is not
 429 meaningful to consider the RMS/WRMS of the UT1-UTC estimates based
 430 on these sessions. This is also the case for the Subset-3. In the following we
 431 focus only on Subset-1 and Subset-2.

Table 4: Number of sessions and corresponding RMS/WRMS of UT1-UTC values w.r.t. C04 for the sessions included in Subset-1.

		L1		L2	
	#Sessions	RMS [μs]	WRMS [μs]	RMS [μs]	WRMS [μs]
W1	1649	22.58	18.39	938.09	18.70
W2	1469	22.32	18.43	805.21	18.82
W3	1493	22.25	18.43	1096.07	18.74

432 The number of extra sessions obtained with the L1-norm is approximately
 433 5 % compared to the L2-norm. The large increase in the RMS values com-
 434 pared to the WRMS values in the L2-norm indicate that the sessions previ-
 435 ously discarded due to high UT1-UTC estimate have correspondingly large

Table 5: Number of sessions and corresponding RMS/WRMS of UT1-UTC values w.r.t. C04 for the sessions included in Subset-2.

	#Sessions	L1		L2	
		RMS [μs]	WRMS [μs]	RMS [μs]	WRMS [μs]
W1	85	18.83	22.54	3934.66	4130.73
W2	66	17.11	19.38	3280.11	3797.42
W3	67	19.48	19.55	2646.68	5173.04

436 formal errors. Thus, they are heavily downweighted in the WRMS of the
 437 UT1-UTC for all three weighting strategies. Comparing the results from the
 438 L2-norm approach presented in Tables 4 and 2 one can see that the WRMS
 439 values for the L2-norm in Subset-1 are slightly larger.

440 Overall, the greatest contribution of the L1-norm approach is the number
 441 of added sessions, which increase the time resolution of the UT1-UTC series,
 442 rather than the overall accuracy.

443 When we investigate the set of sessions, which pass the outlier filtering
 444 only in the L1-norm approach (see Figure 4), we see a clear difference both
 445 in RMS and WRMS values between the two norms. These values are listed
 446 in Table 5. Now the L2-norm approach produces large values in both RMS
 447 and WRMS values. These WRMS values indicate, that the formal errors of
 448 the UT1-UTC estimates for the extra sessions in the L2-norm have similar
 449 magnitude.

450 5. Conclusions

451 The increased number of sessions that produce good quality UT1-UTC
452 estimates indicate that the L1-norm clearly improves the automated ambi-
453 guity estimation for the INT1 sessions. The improvement provided by the
454 L1-norm is also supported by the generally smaller RMS and WRMS values
455 of the post-fit residuals from the ambiguity estimation. In general the L1-
456 norm approach yields an improvement of 15–20 % in WRMS of the post-fit
457 residuals. The subset of added sessions with respect to the L2-norm approach
458 generally represent an average sample of INT1 sessions. The average number
459 of observations in the sessions which benefited from the L1-norm ambiguity
460 estimation is almost identical to the average number of observations over the
461 whole set of analysed INT1 sessions. This implies that the improvement in
462 ambiguity resolution with the L1-norm is not correlated with particularly
463 high or low number of observations in the sessions.

464 The number of sessions that are improved by the L1-norm approach
465 greatly outnumber the ones where the issues of stability result in a failed
466 ambiguity estimation. Quantitatively, the increase in number of sessions by
467 using the L1-norm is approximately 5 %.

468 The computational complexity of solving the linear programming prob-
469 lem compared to inverting the normal equations does not generally cause
470 significant overhead in the processing time for an individual session. The con-
471 vergence of the L1-norm varied between the different weighting approaches.
472 For the L2-norm the different weighting options behaved more uniformly.
473 However, slow convergence does not necessarily lead to bad quality of the
474 results. Using the W1 weighting, the L1-norm iteration counts were signif-

475 icantly larger compared to those of the L2-norm. However, the L1-norm
476 using the W1 weighting (i.e. equally weighted) produced the biggest increase
477 in good quality UT1-UTC estimates.

478 **Acknowledgements**

479 We would like to acknowledge the IVS (Behrend, 2013) for providing
480 the VLBI databases used in this work. We also would like to thank the
481 two anonymous reviewers for their valuable comments that helped greatly to
482 improve this paper.

483 **References**

- 484 Altamimi, Z., Collilieux, X., Métivier, L., 2011. ITRF2008: an improved
485 solution of the international terrestrial reference frame. *J. Geod.* 85 (8),
486 457–473.
- 487 Amiri-Simkooei, A. R., 2003. Formulation of L_1 norm minimization in Gauss-
488 Markov models. *J. Surv. Eng.* 129 (1), 37–43.
- 489 Andersen, P., 2000. Multi-level arc combination with stochastic parameters.
490 *J. Geod.* 74 (7-8), 531–551.
- 491 Andersen, R., 2008. Modern methods for robust regression. No. 152 in 7.
492 Sage.
- 493 Barnes, R. T. H., Hide, R., White, A. A., Wilson, C. A., 1983. Atmospheric
494 angular momentum fluctuations, length-of-day changes and polar motion.
495 *Proc. R. Soc. London, Ser. A* 387 (1792), 31–73.

- 496 Behrend, D., 2013. Data Handling within the International VLBI Service.
497 Data Sci. J. 12, WDS81–WDS84.
- 498 Bizouard, C., Gambis, D., 2011. IERS C04 08.
499 <https://hpiers.obspm.fr/iers/eop/eopc04/C04.guide.pdf>, the
500 combined solution C04 for Earth Orientation Parameters consistent with
501 International Terrestrial Reference Frame 2008. Accessed: 2016-06-29.
- 502 Böhm, J., Böhm, S., Nilsson, T., Pany, A., Plank, L., Spicakova, H., Teke,
503 K., Schuh, H., 2012. 'The new Vienna VLBI software VieVS'. In: Kenyon,
504 S., Pacino, M. C., Marti, U. (Eds.), *Geodesy for Planet Earth: Proceedings*
505 *of the 2009 IAG Symposium*. Vol. 136. Springer, pp. 1007–1011.
- 506 Bolotin, S., Baver, K., Gipson, J., Gordon, D., MacMillan, D., 2014. 'The
507 VLBI Data Analysis Software ν Solve: Development Progress and Plans
508 for the Future'. In: Baver, K. D., Behrend, D., Armstrong, K. L. (Eds.),
509 *IVS 2014 General Meeting Proceedings "VGOS: The New VLBI Network"*.
510 Science Press, Beijing, pp. 253–257.
- 511 Brzeziński, A., 2012. On estimation of high frequency geophysical signals in
512 Earth rotation by complex demodulation. *J. Geodyn.* 62, 74–82.
- 513 Hobiger, T., Otsubo, T., Sekido, M., Gotoh, T., Kubooka, T., Takiguchi, H.,
514 2010. Fully automated VLBI analysis with c5++ for ultra-rapid determi-
515 nation of UT1. *Earth Planets Space* 62 (12), 933–937.
- 516 Kareinen, N., Hobiger, T., Haas, R., 2015. Automated analysis of Kokee–
517 Wettzell Intensive VLBI sessions—algorithms, results, and recommenda-
518 tions. *Earth Planets Space* 67, 181.

- 519 Koch, K.-R., 1999. Parameter estimation and hypothesis testing in linear
520 models. Springer-Verlag Berlin Heidelberg.
- 521 Lagler, K., Schindelegger, M., Böhm, J., Krasna, H., Nilsson, T., 2013.
522 GPT2: Empirical slant delay model for radio space geodetic techniques.
523 Geophys. Res. Lett. Vol. 40 (6), 1069–1073.
- 524 Ma, C., Sauber J.M., Bell L.J., Clark, T., Gordon, D., Himwich W.E., Ryan
525 J.W., 1990. Measurement of horizontal motions in Alaska using very long
526 baseline interferometry. J. Geophys. Res. 95 (B13), 21991–22011.
- 527 Malkin, Z., Skurikhina, E., 2005. OCCAM/GROSS Software Used at the
528 IAA EOP Service for processing of VLBI Observations. Transactions of
529 the Institute of Applied Astronomy of the RAS 12, 54–67.
- 530 Murty, K. G., 1983. Linear programming. John Wiley & Sons.
- 531 Rogers, A. E., 1970. Very long baseline interferometry with large effective
532 bandwidth for phase-delay measurements. Radio Sci. 5 (10), 1239–1247.
- 533 Titov, O., Tesmer, V., Böhm, J., 2004. 'OCCAM v. 6.0 software for VLBI
534 data analysis'. In: Vanderberg, N. R., Baver, K. D. (Eds.), IVS 2004
535 General Meeting Proceedings. NASA/CP-2004-212255, pp. 267–271.
- 536 Titov, O., Tregoning, P., 2005. Effect of post-seismic deformation on earth
537 orientation parameter estimates from VLBI observations: a case study at
538 Gilcreek, Alaska. J. Geod. 79, 196–202.
- 539 Walt, S., Colbert, S. C., Varoquaux, G., 2011. The NumPy Array: A Struc-
540 ture for Efficient Numerical Computation. Comput. Sci. Eng. 13 (2), 22–30.